Through Glass Via Drilling Using GHz-bursts of Femtosecond Pulses: Challenges and Implementation

Pierre Balage[1], John Lopez [1], Théo Guilberteau [1,2], Manon Lafargue [1,3], Guillaume Bonamis [3], Clemens Hönninger [3], and Inka-Manek-Hönninger [*1]

[1] *University of Bordeaux-CNRS-CEA, CELIA UMR5107, 33400 Talence, France*
[2] *ALPhANOV, rue François Mitterrand, 33400 Talence, France*
[3] *AMPLITUDE, 11 avenue de Canteranne, 33600 Pessac, France*
[*]*Corresponding author's e-mail: inka.manek-honninger@u-bordeaux.fr*

Femtosecond GHz-burst mode laser processing is very appropriate for top-down percussion drilling of blind holes in glasses with very high aspect ratio and outstanding hole quality. There is a big interest in drilling through glass vias for applications in microelectronics. However, our study in GHz-burst mode reveals certain constraints and limits in through glass via drilling concerning the outlet diameter of the holes at the rear surface, which is systematically smaller than expected from the results obtained for blind holes. In order to study this observation for different sample thicknesses, we prepared bevel samples and performed light transmission measurements. Finally, we demonstrate how to overcome these limits and suggest an implementation strategy. These results might be of significant importance for industrial applications of through glass via drilling in GHz-burst mode.
DOI: 10.2961/jlmn.2024.03.2007
Keywords: ultrafast laser processing, GHz-bursts, femtosecond pulses, laser-material interaction, glasses, TGV.

1. Introduction

Over the past twenty years, ultrafast laser technology has significantly advanced various industries owing to its versatility and exceptional abilities in micro-processing of transparent dielectric materials [1]. Numerous applications have been reported, including refractive index change [2], 3D data storage [3-6], writing of waveguides and diffraction gratings [7-10], conducting bottom-up drilling [11,12], and achieving zero-kerf, dust-free glass cutting [13].

Due to their ultra-short interaction time, femtosecond lasers facilitate highly precise and intense energy deposition [14,15]. However, the throughput may fall short of industrial needs due to the very low material removal rate per pulse. To enhance femtosecond laser productivity, spatial beam shaping is a compelling strategy. For instance, Bessel beam shaping has been explored for tasks like glass cutting [13,16-18], nano-hole drilling [19], in-volume nanoscale modifications [20], and high aspect ratio drilling [21,22]. This approach enables elongated, precisely localized, and uniformly distributed energy deposition.

Another method for shaping beams is by temporal means, achieved by distributing the pulse energy into bursts containing multiple femtosecond pulses rather than utilizing a single highly energetic pulse. This approach, known as the burst regime, has primarily been explored in processing metals and semiconductors [23-26]. Several studies indicate that, with the right set of parameters, burst usage can enhance the energy deposition and subsequently increase removal rates. However, studies suggest that using MHz-bursts of femtosecond pulses may not be optimal due to the pulse-to-pulse delay within a burst being longer than the materials' heat relaxation time. To address this, the GHz-burst mode has emerged, featuring a pulse-to-pulse delay comparable to the heat relaxation time in dielectrics [27]. Recent research on GHz-burst processing in dielectrics for milling applications echoes the trends observed in metals and silicon [28-30]. These findings were corroborated by a comparative study on surface ablation in fused silica using both MHz- and GHz-burst regimes [31]. While the removal rate tends to increase with the number of pulses per burst, the surface quality may be compromised [32,33]. It is assumed that GHz-burst interaction relies on a thermal accumulation during the burst due to the high pulse repetition rate. Recent investigations on percussion drilling in glasses and sapphire in GHz-burst mode using pump-probe shadowgraphy and thermal imaging have demonstrated efficient drilling, even at burst fluences where the individual pulses within the burst have fluences lower than the material's ablation threshold [34,35]. This highlights the benefit of controlled thermal accumulation in this processing mechanism. Recent research has also focused on understanding the impact of the energy distribution within GHz-bursts and its effect on the drilling process [36].

In this study, we faced drilling limitations in through via drillings in sodalime as illustrated in Figure 1. The holes are crack-free and feature smooth inner walls up to a certain depth as formerly reported [35]. However, all holes show a narrowing tip towards the outlet diameter at the rear surface regardless of the drilling depth as can be clearly observed on the bevel sample (image on the right) in comparison to blind holes (image on the left). The hole diameters have been measured with an optical microscope. Note that all the holes were drilled with the exact same number of bursts and the same burst fluence and only the hole depth changes with the varying sample thickness thanks to the bevel form of the

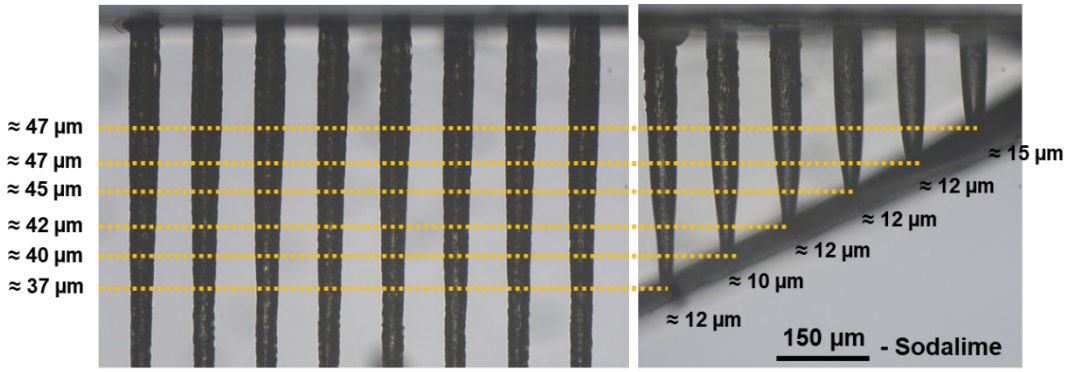

Fig. 1 Microscope images of blind holes (left) and through holes in a bevel sample (right) in sodalime drilled with a repetition rate of 1 kHz and a burst fluence of 390 J/cm².

sample. Based on this observation, we decided to implement a systematic study of light transmission on bevel samples in order to better understand the role of optical transmission and its influence on the drilling result.

This article is organized as follows: Section 2 describes the experimental setup for this study. In section 3, we detail two different protocols for bevel sample preparation and hole drilling. The transmission measurements are described in section 4, followed by a discussion (section 5) and a conclusion (section 6).

2. Experimental setup

We used an Yb-doped 100 W femtosecond laser system based on a Tangor 100 from Amplitude emitting pulses at 1030 nm with a pulse duration of 500 fs. The laser can be operated in Single Pulse regime, MHz-burst regime at 40 MHz- as well as GHz-burst regime at 1.28 GHz.

During this study, we used two different micromachining workstations. The first one is a glass cutting workstation, used to prepare the bevel samples, based on a Bessel beam module described in [37]. The latter, by means of an axicon allows us to generate a primary Bessel beam with high dimensions and therefore a low fluence. This primary Bessel beam is unable to generate non-linear absorption in the material and thus it does not generate a pre-cut plane. Therefore, we use a telescope-like system based on two lenses f_1=125 mm and f_2 = 10 mm for a resulting demagnification coefficient of 12.5. This telescope-like system creates a secondary Bessel beam with much lower dimensions, and thus a higher fluence, that can generate a pre-cut plane. The cutting process here requires two steps. The first one being the pre-cutting of the sample by translating the sample into the Bessel beam. Then, in a second time, it is possible to separate the pieces by applying a slight mechanical force.

The second workstation is a percussion drilling workstation as described in [34]. This workstation allows us to precisely drill the materials with an excellent repeatability. It is also partially automatized with the DMC PRO software in order to perform several similar experiments for data robustness. This workstation uses a microscope objective (Mitutoyo, model APO NIR x5/NA 0.14) in order to focalize the laser beam on the sample. The resulting spot size with this setup was measured using a beam analyser (DataRay, WinCamD-XHR, pixel size 3.3 µm) coupled with a homemade calibrated magnification system to 8.5 µm for a numerical aperture of 0.14. It is also equipped with a white light system coupled with two dichroic mirrors so that we can visualize the sample directly through the focalization head in order to optimize the focus position with a camera. The latter, along with the autofocus function from DMC PRO allows for a high reproducibility. The focusing head also allows us to optimize the position of the spot regarding the inlet of the holes in the transmission measurements. Moreover, we mounted a sideview imaging system with a green diode, an InfiniMax long distance microscope and a CMOS camera to observe the process. We added a green filter with a bandwidth of 10 nm upstream the camera in order to not being blinded by the processing wavelength.

Both these workstations are schematically represented in Figure 2. These stations are both mounted on granite

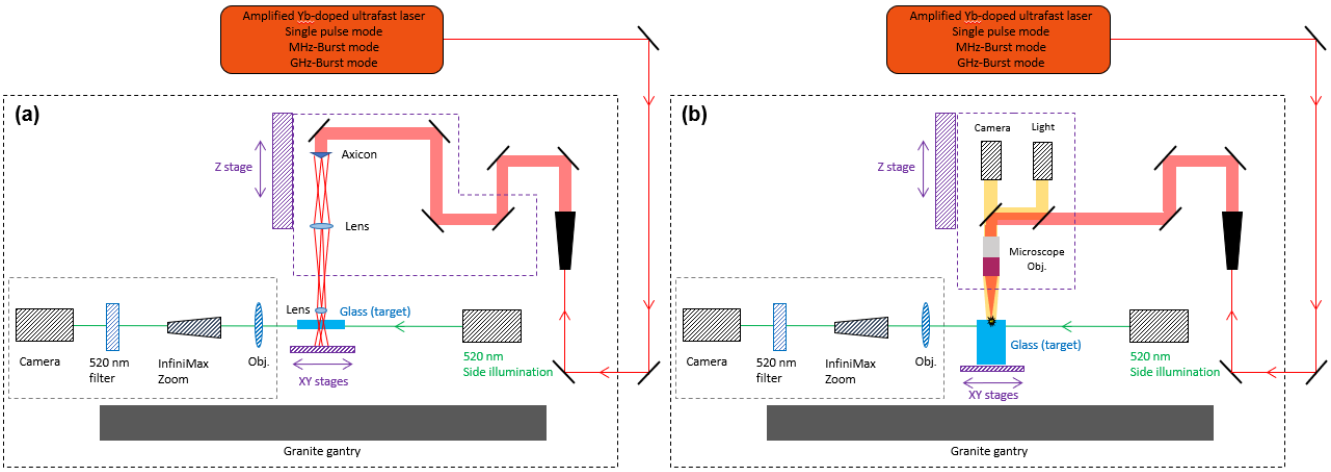

Fig. 2 Schematic representation of the workstation for glass cutting with a Bessel beam (a) and the percussion drilling workstation (b).

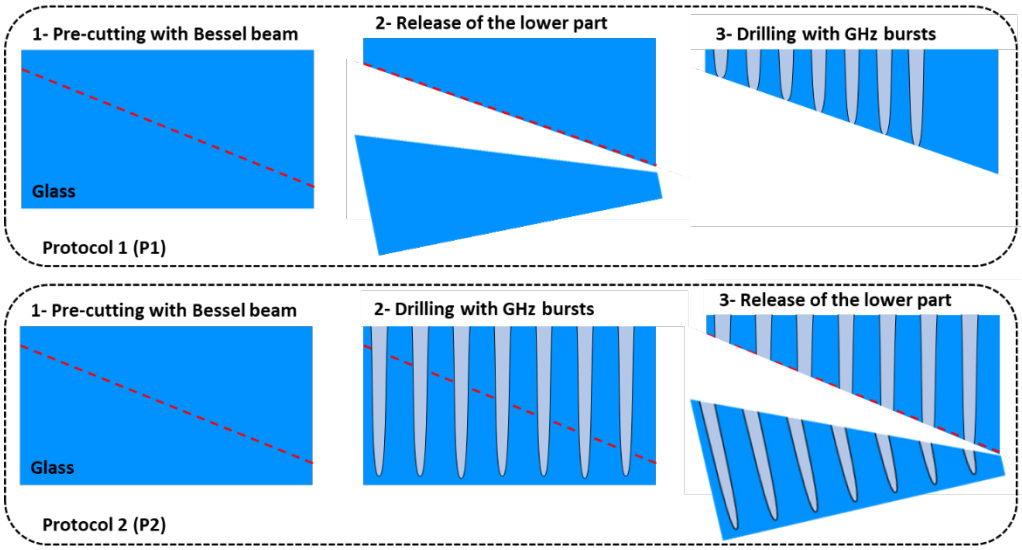

Fig. 3 Schematic representation of the two protocols used for sample preparation.

gantries to ensure the stability and the reproducibility of the experiments.

3. Sample preparation

In order to provide an extensive study on different depths of through holes on a single sample, we decided to use bevel samples as reported in literature [38]. We used the two above mentioned workstations, the first one to pre-cut a bevel sample out of a rectangular sample with the Bessel beam configuration, and then, the second one to drill holes in GHz-burst mode with a focused Gaussian beam.

The samples were prepared along two different protocols as schematically represented in Figure 3. First, the protocol (P1) for this experiment consists in the following three steps:

- Pre-cutting of bevel samples by means of the Bessel beam workstation.
- Part release with a slight mechanical stress.
- Drilling of the bevel sample in GHz-burst mode. Every hole is drilled with the exact same parameters. We chose a burst repetition rate of 1 kHz and the maximum fluence so that we could drill a sufficient number of holes with increasing depth in a single sample. The drilling time is fixed at 10 s.

The second protocol was designed in order to increase the outlet diameter following the observations made on Figure 1. On the basis of this observation, we defined a new protocol (P2) including three steps in order to measure the optical transmission in blind hole drilling conditions (with large outlet diameters). The new protocol (P2) is:

- Pre-cutting of bevel samples by means of the Bessel beam workstation.
- Drilling of the bevel sample in GHz-burst mode. Every hole is drilled with the exact same parameters. We chose a burst repetition rate of 1 kHz and the maximum fluence so that we could drill a sufficient number of holes with increasing depth in a single sample. The drilling time is fixed at 10 s.
- Part release with a slight mechanical stress.

During the procedure, for releasing the pre-cut part, it is possible to use an airgun to replace the mechanical stress. This allows for releasing the lower part without touching the sample. However, this was only possible with sodalime samples and did not work on fused silica. The bevel samples were prepared by means of our Bessel beam cutting module which allowed us to pre-cut 1 mm thick samples of sodalime and fused silica. The drilling was realised with GHz-bursts of 50 pulses at 1.28 GHz with a burst repetition rate of 1 kHz and a burst fluence of 400 J/cm². The drilling time was fixed at 10 s for all holes. The bevel samples obtained with both protocols in sodalime are depicted in Figure 4 (a) and (b). Figure 4 (c) displays the bevel sample obtained in fused silica for Protocol 1.

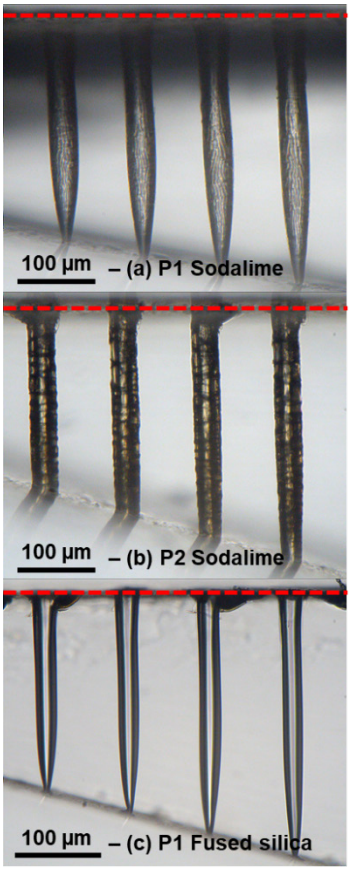

Fig. 4 Bevel sample obtained from Protocol 1 (a) and Protocol 2 (b) in sodalime, and from Propotocl 1 (c) in fused silica.

Unfortunately, in fused silica we were not able to implement Protocol 2 as it was impossible to release the lower part of the drilled sample without breaking the whole bevel. However, we would have expected the transmission to follow the same tendency as the morphology of the hole is constant in this case and corresponds to the holes published in [35]. Thanks to Protocol 2 in sodalime, we were able to significantly increase the outlet diameter of the hole. This observation suggests that the ablation plume has a major role in the drilling process and especially in the enlargement of the hole diameter.

To keep the outlet diameter comparable to the expected one, it is important to keep some material underneath the desired depth.

However, by this means only the upper, crackled part of the hole is kept. Therefore, we expect to observe a decrease of the transmission for these holes. A point worth noticing here is that, although the drilling parameters are exactly the same, the holes drilled along protocol (P1) do not display cracks at the inlet of the hole. This peculiar behavior will be discussed in section 5. Note that the pre-cutting by a Bessel beam had no influence on the drilling result. Indeed, the obtained holes correspond perfectly to former observations on GHz-burst drilling as reported in [35].

4. *Post-mortem* transmission measurement

After drilling the hole series in GHz-burst mode according to Protocols 1 and 2 as just described in Section 3 we analyzed the holes in the different bevel samples by post-mortem light transmission measurements with a photodiode as schematically depicted in Figure 5.

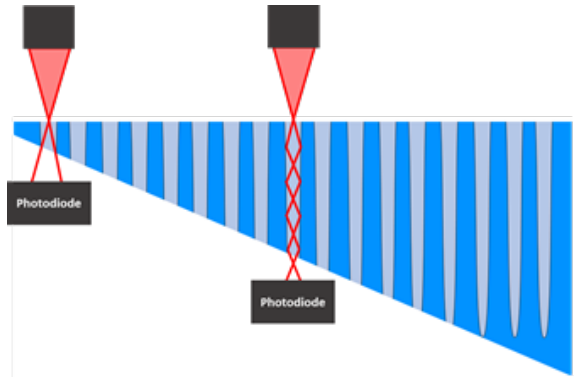

Fig. 5 Schematic representation of the transmission measurement.

During these measurements, two main challenges emerged, the first one is related to the detector position, and the second one to the light source to be used. Indeed, concerning the detector position one has to find a compromise for properly placing the photodiode not touching the sample, but close enough to collect as much transmitted light as possible. The second challenge was the light source itself. We operated the laser in MHz-burst mode with a burst fluence lower than the single-pulse ablation threshold for the post-mortem transmission measurements. In this configuration it was possible to place the spot right at the inlet of the hole by repositioning the sample accurately. The correct position of the spot could be determined with a precision close to the micrometre by moving the sample at the position corresponding to the maximum power on the photodiode. Note, the repetitive single pulse mode could not be used for the transmission measurements as the high intensity of the pulses was able to ionize the air and thus causing the risk of eventually degrading the quality and the trueness of the measurement. Moreover, the GHz-burst mode laser could not be used either as its micromachining efficiency is too high. Indeed, when the laser spot was misplaced by only a few micrometres, the light starts to modify the inlet of the hole and thus changing the aspect ratio and consequently the light transmission.

The resulting graphs are depicted on Figure 6 (a) where we display the evolution of the transmission as a function of the hole depth for the two protocols investigated in sodalime. The photodiode we used (Gentec, PH20-GD-D0) has an upper limit of 30 mW, we estimated the uncertainty on the transmission measurement to be about 10 % but we did not represent it on the graph for the sake of clarity.

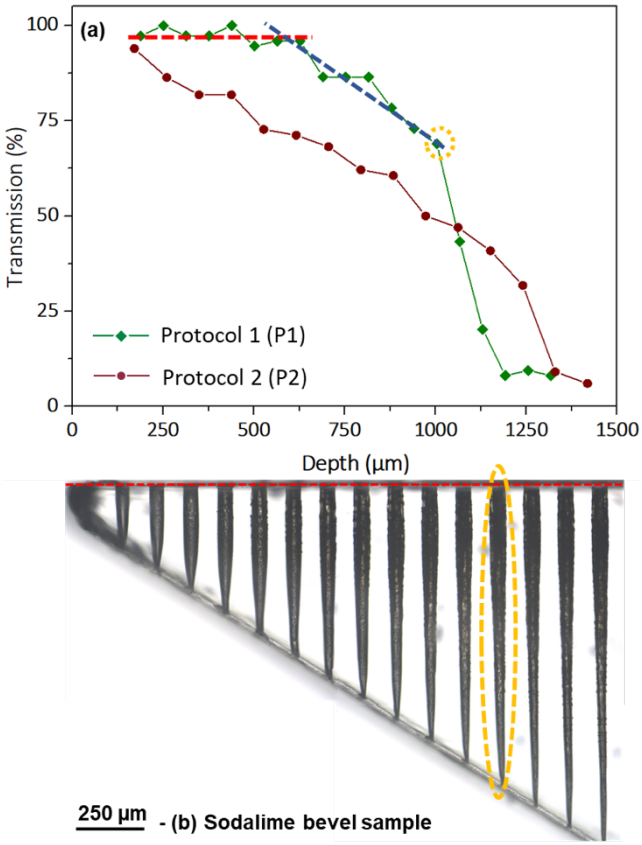

Fig. 6 Transmission of the hole as a function of its depth for both protocols (a). Microscope image of the holes obtained on sodalime with Protocol 1 and a burst fluence of 400 J/cm² at a repetition rate of 1 kHz (b).

On this graph, one can observe that the two curves are considerably different. The green curve, corresponding to protocol P1, seems to display a threshold beyond which the transmission drops significantly from nearly 75 % to 7%. The red curve corresponding to protocol P2 displays a quasi-linear decrease of the transmission as a function of the depth. As was expected in this case, the transmission decreases as the hole goes deeper. Note that, the cracks appearing in the first few hundreds of micrometres of the hole significantly affect the transmission. Indeed, even for short holes, the transmission in the red curve is lower than that was observed on the green curve.

For Protocol 1 (P1), in order to get a better sense of the phenomenon occurring here, it is important to have a look at

the hole morphology as depicted on Figure 6 (b). This image of the bevel sample taken with the microscope allows us to observe the very same morphology as the one observed in Figure 4 (a). On the graph displayed on Figure 6 (a) we inserted two linear fits as a visual guide for our hypothesis.

The first line in dashed red corresponds to the first stage of the drilling. In this case the plume expands freely in the air and its kinetic energy allows it to be fully ejected from the hole. In this case, the transmission of the hole is rather constant and close to 100 % up to a depth of approximatively 450 µm, which is much higher than the confocal parameter (about 100 µm), so we expect highly efficient reflection under grazing incidence on smooth inner walls (see Fig. 4 (a)). For deeper holes, we observe that the transmission drop corresponds to the appearance of cracks in the upper part of the hole. We assume that the alteration of the inner walls for longer holes results from either the interaction between the ablation plume and inner walls (high temperature, mechanical erosion…) or the absorption of the incoming laser beam by redeposited matter on the inner walls. This phenomenon does not occur in the beginning of the drilling as the kinetic energy of the plume is high enough so that it can fully escape the hole. However, to fully explain this observation further studies are necessary.

Then we get to the hole circled in dashed yellow. This hole corresponds to a certain threshold beyond which the transmission drops significantly. We suppose that this point corresponds to the depth for which the fluence at the tip of the hole is getting closer to the threshold beyond which the drilling is over. Therefore, we expect that the drilling rate slows down from this point. Note that the three last points in green correspond to holes that are not through.

It is worth noticing that, in our case, we implemented a *post-mortem* transmission measurement in the MHz-burst regime. Although the *post-mortem* measurements give us a good idea of the transmission evolution with increasing hole depth, one should keep in mind the fact that the absorption of the laser beam along the hole could be slightly different during the drilling process since (i) the laser intensity is lower in the GHz-burst regime, (ii) the confined plume may absorb part of the incoming laser pulse, and (iii) both inner walls morphology and hole geometry change during the drilling process.

In fused silica, the hole morphology is very different since the inner walls are smoother, so we expect a higher transmission of the hole. In addition, the inner walls' quality does not change during the drilling. Therefore, we expect to observe less variations in the transmission. The microscope image of the bevel sample and the corresponding transmission measurement are displayed in Figure 7.

On this figure we can notice that the inlet diameter in fused silica is significantly lower than in sodalime due to the higher ablation threshold in fused silica [39], which increased the difficulty of putting the spot back into the hole for the transmission measurements. On this graph, we can see that the evolution of the transmission as a function of the hole depth is different than that was observed in sodalime.

In the case of fused silica, we can observe that the transmission for the Protocol 1 evolves rather similarly to what was observed for Protocol 2 in sodalime with a single negative slope. In fused silica the transmission is in general much higher, attesting that its very high hole quality is beneficial for the transmission (1.1 % losses per 100 µm compared to 5 % in sodalime). In the particular case of fused silica, the transmission drop is then basically only due to refraction losses and almost no scattering occurs.

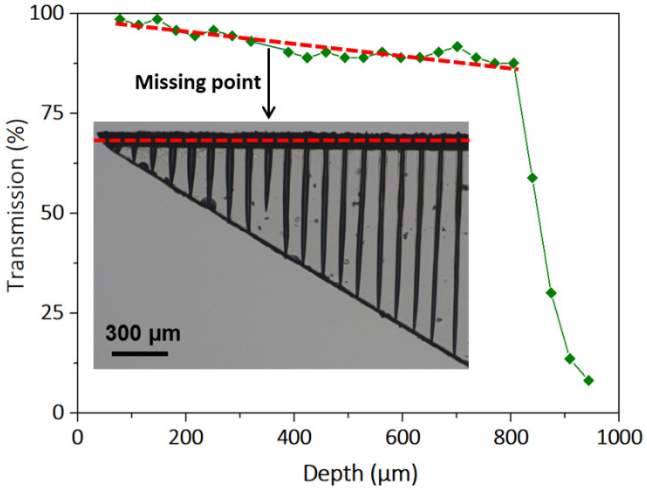

Fig. 7 Transmission of the hole as a function of its depth for Protocol 1 along with the microscope image of the holes in fused silica for a burst fluence of 400 J/cm² at a repetition rate of 1 kHz.

The missing point in the transmission measurement corresponds to the blind hole visible on the microscope image (insert). It might be due to a small dust particle on the front surface of the sample as fused silica is very sensitive to the front surface conditions for GHz-burst drilling.

5. Discussion

In Figure 4 (a), it appeared that the uncracked zone near the tip of the hole was rather constant. This means that the crackling appearing in sodalime is most likely due to some redeposited matter from the ablation plume or to the ablation plume-inner walls interaction that changes the absorption and scattering of the inner walls. The last 200 µm of the hole are always smooth due to the fact that no matter is redeposited here as the kinetic energy of the plume allows for a matter redeposition further upstream.

On Figure 6 (b), the cracks on the first part of the hole appear at a certain hole depth, roughly 400 µm. In the case of the first protocol, the first holes do not display cracks in the first part of the hole. Indeed, as soon as the plume escapes the hole by the outlet, the drilling is over and hence there is no material redeposited on the inner walls anymore, nor ablation plume-inner walls interaction. As a consequence, the transmission remains high as the inner walls are smooth. Once the depth reaches a certain value, prior to the hole goes through, the depth is already too high for the plume to escape, cracks begin to appear leading to a slight decrease in the transmission. This assumption can be confirmed by the fact that the length of the smooth zone at the tip of the hole, identified on Figure 4, is more or less constant for a constant burst energy.

We assume that as soon as the hole goes through, the drilling is over, no matter the number of bursts applied after, the burst fluence or the repetition rate. From several real-time sideview observations during the through hole drilling process, it appeared that the drilling stops as soon as the ablation plume leaves the hole (i.e. as soon as the hole goes through),

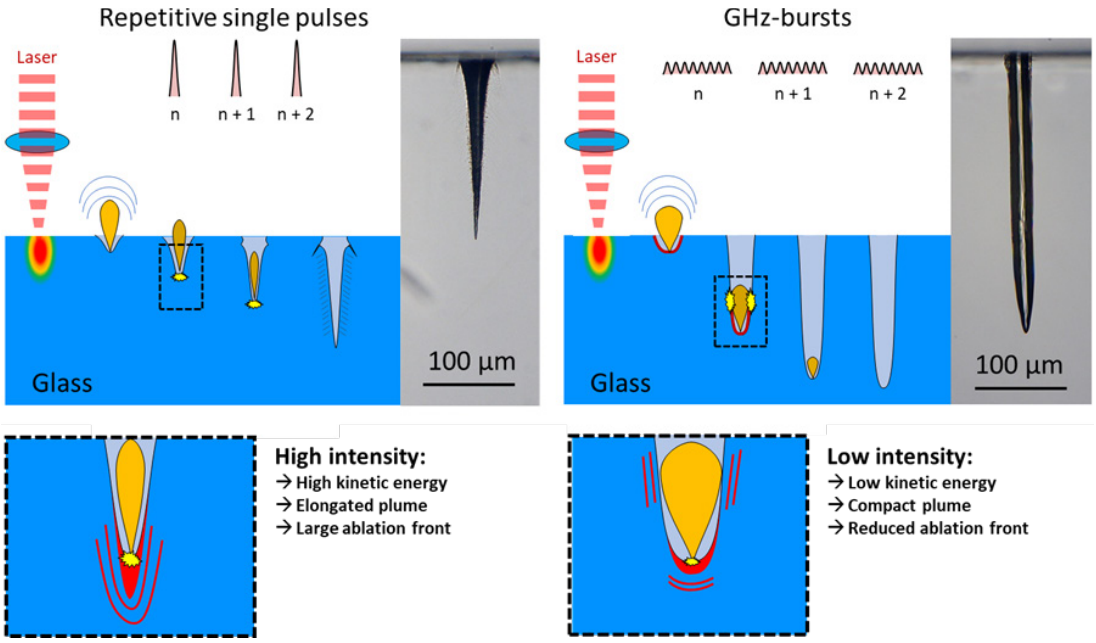

Fig. 8 Schematic representation of the drilling process in the repetitive single pulse regime and in the GHz-burst mode.

leaving an outlet diameter of around 8 µm. This observation could mean that the enlargement of the hole diameter during the drilling, leading to cylindrical holes, might come from the ablation plume itself in the GHz-burst regime. On the basis of this observation, we assume that the drilling mechanisms between the repetitive single pulse regime and the GHz-burst are fully different as depicted in Figure 8. The former is based on direct laser ablation. The ablation rate is high at the very tip of the hole due to high effective fluence whereas the ablation rate is low on inner walls due to a low fluence (close to the ablation threshold). A low ablation of the inner walls explains the slight enlargement of the hole during the drilling process resulting in a conical morphology. On the contrary, in the case of GHz-bursts, the drilling mechanism at the bottom of the hole results mainly from the heat accumulation brought by the high pulse repetition rate and the elevated number of pulses per burst. The enlargement of the hole is not provoked by direct laser ablation anymore but by the interaction between the plume (which is composed of hot dense matter) and the inner walls either by mechanical erosion or by heat transfer. So, without the plume, there is no enlargement of the hole.

6. Conclusion

In this paper, we investigated the evolution of the optical transmission of holes drilled with GHz-bursts of femtosecond pulses as a function of their depth via two designed protocols in sodalime glass and fused silica. We also provided experimental evidences that the inner walls' quality has an impact on the transmission of the holes, and thus on the drilling process, which tends to confirm our hypothesis that high aspect ratios are achievable in GHz-burst mode thanks to the guiding of the laser beam by the hole itself. Structured and slightly cracked inner walls observed in sodalime glass can be correlated to relatively high optical transmission losses due to scattering (about 5 % per 100 µm) whereas glossy inner walls obtained in fused silica lead to clearly lower optical transmission losses (about 1.1 % per every 100 µm).

Although blind and through holes are drilled with the same set of operating parameters and the same number of GHz-bursts, they exhibit quite different geometries and exit diameters. It is worth noticing that once the hole reaches the rear surface opening a through via, the geometry and the diameter of this hole stop evolving. Therefore, we assume that the ablation plume contributes to enlarge the exit hole, and thus, plays a major role on the final hole geometry and exit diameter. This limitation can be overcome using a sacrificial layer directly underneath the sample as shown in [40]. This assumption led us to believe that bottom-up drilling might not be possible in the GHz-burst regime as the plume would immediately be ejected from the rear side of the sample.

These experiments constitute a first step in the seek for a better understanding of the GHz-burst regime for laser processing.

References

[1] G. Račiukaitis: IEEE J. Sel. Top. Quantum Electron., 27, (2021) 1100112.
[2] D. Homoelle, S. Wielandy, A. L. Gaeta, N. F. Borrelli, and C. Smith: Opt. Lett., 24, (1999) 1311.
[3] S. Juodkazis, S. Matsuo, H. Misawa, V. Mizeikis, A. Marcinkevicius, H.-B. Sun, Y. Tokuda, M. Takahashi, T. Yoko, and J. Nishii: Appl. Surf. Sci., 197–198, (2002) 705.
[4] M. H. Hong, B. Luk'yanchuk, S. M. Huang, T. S. Ong, L. H. Van, and T. C. Chong: Appl. Phys. A: Mater. Sci. Process., 79, (2004) 791.
[5] E. N. Glezer, M. Milosavljevic, L. Huang, R. J. Finlay, T. -H. Her, J. P. Callan, and E. Mazur: Opt. Lett., 22, (1997) 422.
[6] A. Marcinkevičius, S. Juodkazis, M. Watanabe, M. Miwa, S. Matsuo, H. Misawa, and J. Nishii: Opt. Lett., 26, (2001) 277.
[7] K. Minoshima, A. M. Kowalevicz, I. Hartl, E. P. Ippen, and J. G. Fujimoto: Opt. Lett., 26, (2001) 1516.

[8] C. B. Schaffer, A. Brodeur, J. F. García, and E. Mazur: Opt. Lett., 26, (2001) 93.
[9] K. M. Davis, K. Miura, N. Sugimoto, and K. Hirao: Opt. Lett., 21, (1996) 1729.
[10] K. Minoshima, A. Kowalevicz, E. Ippen, and J. Fujimoto: Opt. Express, 10, (2002) 645.
[11] K. Mishchik, K. Gaudfrin, and J. Lopez: J. Laser Micro Nanoeng., 12, (2017) 321.
[12] J. Lopez, S. Niane, G. Bonamis, P. Balage, and I. Manek-Hönninger: J. Laser Micro Nanoeng., 17, (2022) 50.
[13] K. Mishchik, R. Beuton, O. Dematteo Caulier, S. Skupin, B. Chimier, G. Duchateau, B. Chassagne, R. Kling, C. Hönninger, E. Mottay, and J. Lopez: Opt. Express, 25, (2017) 33271.
[14] B. N. Chichkov, C. Momma, S. Nolte, F. yon Alvensleben, and A. Tünnermann: Appl. Phys. A, 63, (1996) 109.
[15] K. Sugioka and Y. Cheng: Light Sci Appl, 3, (2014) e149.
[16] S. Nisar, L. Li, and M. A. Sheikh: J. Laser Appl., 25, (2013) 042010.
[17] R. Meyer, R. Giust, M. Jacquot, J. M. Dudley, and F. Courvoisier: Appl. Phys. Lett., 111, (2017) 231108.
[18] B. N. M. Jenne, D. Flamm, T. Ouaj, J. Hellstern, J. Kleiner, D. Grossmann, M. Koschig, M. Kaiser, M. Kumkar, and S. Nolte: Opt. Lett., 43, (2018) 3164.
[19] M. K. Bhuyan, F. Courvoisier, P. A. Lacourt, M. Jacquot, R. Salut, L. Furfaro, and J. M. Dudley: Appl. Phys. Lett., 97, (2010) 8.
[20] J. Del Hoyo, R. Meyer, L. Furfaro, and F. Courvoisier: Nanophotonics, 10, (2021) 1089.
[21] S. Mitra, M. Chanal, R. Clady, A. Mouskeftaras, and D. Grojo: Appl. Opt., 54, (2015) 7358.
[22] Y. V. White, X. Li, Z. Sikorski, L. M. Davis, and W. Hofmeister: Opt. Express, 16, (2008) 14411.
[23] C. Kerse, H. Kalaycoglu, P. Elahi, B. Cetin, D. Kesim, O. Akçaalan, S. Yavas, M. Asik, B. Oktem, H. Hoogland, R. Holzwarth, and F. O. Ilday: Nature, 537, (2016) 84.
[24] T. Hirsiger, M. Gafner, S. Remund, M. V. Chaja, A. Urniezius, S. Butkus, and B. Neuenschwander: Proc. SPIE, Vol. 11267, (2020) 112670T.
[25] O. Balachninaite, V. Tamulienė, L. Eičas, and V. Vaičaitis: Results Phys., 22, (2021) 103847.
[26] D. J. Förster, B. Jaeggi, A. Michalowski, and B. Neuenschwander: Materials, 14, (2021) 3331.
[27] R. Gattass and E. Mazur: Nat. Phot., 2, (2008) 219.
[28] S. Schwarz, S. Rung, C. Esen, and R. Hellmann: Opt. Lett., 46, (2021) 282.
[29] S. M. Remund, M. Gafner, M. V. Chaja, A. Urniezius, S. Butkus, and B. Neuenschwander: Procedia CIRP, 94, (2020) 850.
[30] S. Hendow, H. Takahashi, and M. Yamaguchi, J. Z. Xu: Proc. SPIE 11268, (2020) 1126809.
[31] D. Metzner, P. Lickschat, C. Kreisel, T. Lampke, and S. Weißmantel: Appl. Phys. A, 128, (2022) 637.
[32] A. Zemaitis, M. Gaidys, P. Gečys, M. Barkauskas, and M. Gedvilas: Opt. Express, 29, (2021) 417883.
[33] F. Caballero-Lucas, K. Obata, and K. Sugioka: Int. J. Extreme Manuf. 4, (2022) 015103.
[34] J. Lopez, S. Niane, G. Bonamis, P. Balage, E. Audouard, C. Hönninger, E. Mottay, and I. Manek-Hönninger: Opt. Express, 30, (2022) 12533.
[35] P. Balage, J. Lopez, G. Bonamis, C. Hönninger, and I. Manek-Hönninger: Int. J. Extreme Manuf., 5, (2023) 015002.
[36] P. Balage, G. Bonamis, M. Lafargue, T. Guilberteau, M. Delaigue, C. Hönninger, J. Qiao, J. Lopez, and I. Manek-Hönninger : Micromachines, 14, (2023) 1158.
[37] P. Balage, T. Guilberteau, M. Lafargue, G. Bonamis, C. Hönninger, J. Lopez, and I. Manek-Hönninger: Micromachines, 14, (2023) 1650.
[38] S. Lazare, J. Lopez, and F. Weisbuch: Appl. Phys. A, 69, (1999) 1.
[39] D. Nieto, J. Arines, G. M. O'Connor, and M. T. Flores-Arias: Appl. Opt., 54, (2015) 8596.
[40] P. Balage, J. Lopez, M. Lafargue, T. Guilberteau, G. Bonamis, C. Hönninger, and I. Manek-Hönninger : Proc. SPIE, Vol. 13005, (2024) 1300504.

(Received: June 10, 2024, Accepted: October 27, 2024)